Walther, W. D. Philips, and D. Kleppner, Phys. Rev. Lett. **28,** 1159 (1972).

[2]H. Grotch and R. A. Hegstrom, Phys. Rev. A 4, 59 (1971), and references therein.

[3](a) W. Perl and V. Hughes, Phys. Rev. **91,** 842 (1953); (b) W. Perl, Phys. Rev. **91,** 852 (1953); (c) A. Abragam and J. H. Van Vleck, Phys. Rev. **92,** 1448 (1953);(d) J. O. Hirshfelder, C. F. Curtiss, and R. B. Bird, *Molecular Theory of Gases and Liquids* (Wiley, New York, 1954), p. 1044; (e) V. W. Hughes, in *Recent Research in Molecular Beams,* edited by I. Estermann (Academic, New York, 1959).

[4]Private communication by B. Zak and work reported by J. Brossel at the Third International Conference on Atomic Physics, Boulder, Colorado, August, 1972.

[5]See, for example, J. J. Sakurai, *Advanced Quantum Mechanics* (Addison-Wesley, Reading, Mass., 1967), p. 109.

[6]G. Breit, Phys. Rev. **34,** 553 (1929).

[7]S. J. Brodsky and J. R. Primack, Ann. Phys. (N.Y.) **52,** 315 (1969).

[8]G. W. Erickson and D. R. Yennie, Ann. Phys. (N.Y.) **35,** 271 (1965).

[9]S. J. Brodsky and R. G. Parsons, Phys. Rev. **163,** 134 (1968).

[10]H. Araki, Prog. Theor. Phys. **17,** 619 (1957).

[11]H. Grotch, private communication; H. Grotch and R. Kashuba, Phys. Rev. A 7, 78 (1973).

[12]W. E. Lamb, Jr., Phys. Rev. 85, 259 (1952).

[13]See, for example, H. Margenau and G. M. Murphy, *The Mathematics of Physics and Chemistry,* 2nd ed. (Van Nostrand, Princeton, N. J., 1956), p. 411.

[14]Z. V. Chraplyvy, Phys. Rev. **91,** 388 (1953); Phys. Rev. **92,** 310 (1953); W. A. Barker and F. N. Glover, Phys. Rev. **99,** 317 (1955).

[15]H. A. Bethe and E. E. Salpeter, *Quantum Mechanics of One- and Two-Electron Atoms* (Springer, Berlin, 1957), p. 194. See also J. A. Young and S. A. Bludman, Phys. Rev. **131,** 2326 (1963); K. M. Case, Phys. Rev. **95,** 1323 (1954).

[16]M. Phillips, Phys. Rev. **76,** 1803 (1949).

PHYSICAL REVIEW A VOLUME 7, NUMBER 2 FEBRUARY 1973

Linear Polarization of Low-Energy-Electron Bremsstrahlung*

Robert W. Kuckuck and Paul J. Ebert

Lawrence Livermore Laboratory, University of California, Livermore, California 94550

(Received 9 October 1972)

The linear polarization of bremsstrahlung from thin targets ($\sim 50\ \mu g/cm^2$) of Al, Cu, Ag, and Au was measured for incident electron energies of 50, 75, and 100 keV. The polarization was measured as a function of photon energy at four emission angles ($\theta = 22.5°$, 45°, 90°, and 135°). Data presented were obtained with a Compton polarimeter having a large asymmetry ratio (from 35 to 150) and high resolution. The results have been found to be in general agreement with the predictions of various bremsstrahlung calculations.

I. INTRODUCTION

Bremsstrahlung exhibits linear polarization. Several calculations[1-4] of the polarization of electron bremsstrahlung have been carried out since the original nonrelativistic theory of Sommerfeld[5] was published. The most recent work is the relativistic calculation by Tseng and Pratt,[6] which covers the incident electron energy range of 5 keV to 1 MeV. Most calculations have been for single electron interactions and must be compared to experimental results obtained using very thin targets. Most measurements of linear polarization at low energies have been made using relatively thick targets.[7-18] Furthermore, when thin targets were employed, quantitative data were obtained only in limited spectral regions because x-ray detectors of relatively poor resolution were used.[19-26]

For bremsstrahlung, the linear polarization P is defined by the expression

$$P(T_0, k, \theta, Z) = \frac{I_\perp(T_0, k, \theta, Z) - I_\parallel(T_0, k, \theta, Z)}{I_\perp + I_\parallel}\ , \tag{1}$$

where $I_\perp$ is the bremsstrahlung intensity component with polarization perpendicular to the reaction plane (the plane containing the direction vectors of both the incident electron and the photon), and $I_\parallel$ is the bremsstrahlung intensity component with polarization parallel to the reaction plane. $I_\perp$, $I_\parallel$, and, therefore, P are functions of electron energy T_0, photon energy k, emission angle θ, and target atomic number Z.

This paper reports measurement of the linear polarization of low-energy bremsstrahlung as a function of k for (a) incident electron energies of 50, 75, and 100 keV, (b) emission angles of 22.5°, 45°, 90°, and 135°, and (c) target atomic numbers of 13, 29, 47, and 79. The measurements were obtained using thin solid targets and a high-resolution Compton polarimeter.

II. EXPERIMENTAL

Apparatus

Part of the experimental arrangement is shown schematically in Fig. 1. The electron beam from a 150-kV accelerator was momentum analyzed and focused to a 5-mm-diam spot on target. The target chamber was a hollow right-circular cylinder of Al, 15 cm long and 10 cm in diam. A 2.54-cm-high Be x-ray port 47 mg/cm^2 thick, subtended

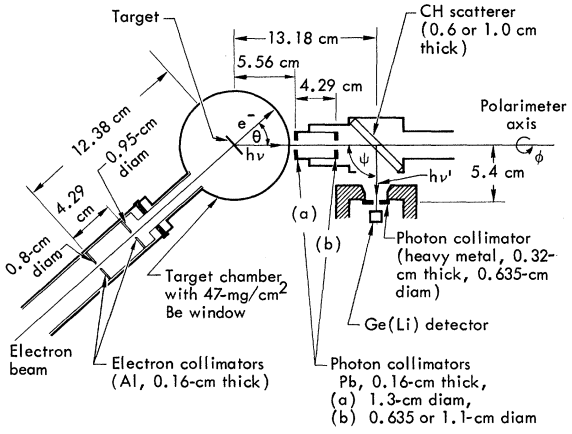

FIG. 1. Schematic drawing of bremsstrahlung target chamber and Compton polarimeter.

265° of polar angle and allowed continuous selection of the bremsstrahlung emission angle from +110° to −155°. The chamber was electrically isolated from ground to serve as a Faraday cup. Beam current was 5 μA or less and was integrated by a commercially available integrator.

The targets were Al (50±5 μg/cm^2), Cu (52±5 μg/cm^2), Ag (38±4 μg/cm^2), and Au (38±4 μg/cm^2). They were prepared by vacuum deposition onto parylene substrates between 5 and 10 μg/cm^2 thick. Average target thickness was determined to within 10% both by weighing and by fluorescent x-ray analysis. To measure background, a parylene substrate was bombarded by an amount of charge equal to that of the corresponding signal run.

The bremsstrahlung and characteristic x rays from the target were collimated before entering the polarimeter, which consisted of an amorphous plastic scatterer and a Ge(Li) spectrometer. After scattering in the plastic, the x rays were detected by the Ge(Li) spectrometer positioned alternately in the emission plane and the plane perpendicular to the emission plane. This was done by rotating the polarimeter about the collimator axis. The scatterer was housed in an air-tight tubular chamber with 0.6-mg/cm^2 Mylar entrance and exit windows. Helium was continually flowed through the chamber to reduce attenuation of low-energy photons. Scatterer thicknesses of 0.6 and 1.0 cm and defining collimator diams of 0.635 and 1.11 cm were used to optimize the count rate, which ranged from 3 to 200 per sec. The planar Ge(Li) spectrometer had an active area of 0.90 cm^2 and a depletion depth of 1.02 cm. Its resolution was 550 eV for the 59.5-keV γ ray from ^{241}Am.

The characteristics of the polarimeter (efficiency, asymmetry ratio, and energy response) were calculated.[27] Of particular importance is the asymmetry ratio $R(k)$ since it determines the sensitivity of the polarimeter to photon polarization and relates the measured spectra to P. $R(k)$ is given by

$$R(k)=\frac{\epsilon(k,\ \psi=\frac{1}{2}\pi,\ \phi=\frac{1}{2}\pi)}{\epsilon(k,\ \psi=\frac{1}{2}\pi,\ \phi=0)}\ , \tag{2}$$

where $\epsilon(k, \psi, \phi)$ is the efficiency of the polarimeter for scattering and detecting a completely polarized beam of monoenergetic photons with the detector at a polar angle ψ with respect to the beam direction, and at an angle ϕ with respect to the plane of polarization. It follows that

$$P(k)=\frac{R(k)+1}{R(k)-1}\ \frac{N_{\parallel}(k)-N_{\perp}(k)}{N_{\parallel}(k)+N_{\perp}(k)}\ , \tag{3}$$

where $N_{\parallel}(k)$ is the number of scattered photons detected by the Ge(Li) spectrometer located in the emission plane and $N_{\perp}(k)$ is the number of scattered photons detected by the Ge(Li) spectrometer located perpendicular to the emission plane. For the scatterer-spectrometer geometries used in the experiment, R ranged from 35 to 150, depending upon photon energy. The polarimeter energy resolution is exhibited in Fig. 2 both by the widths of the more intense L lines of Au and by the sharp cutoff at the bremsstrahlung end-point energy.

Data Analysis

Scattered spectra were recorded in a pulse-height analyzer, stored on magnetic tape, and sub-

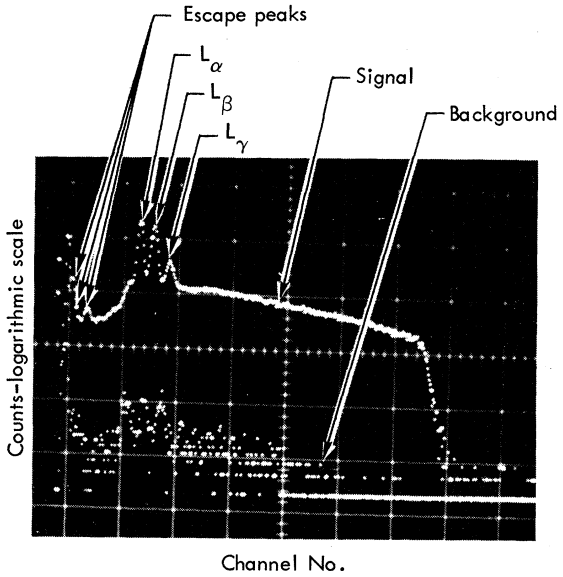

FIG. 2. Photograph of scattered spectrum showing signal and background levels for $T_0=50$ keV, $Z=79$, $\theta=135°$, and polarimeter positioned parallel to reaction plane. Ordinate scale is logarithmic: each division is approximately a factor of 10.

sequently analyzed using a CDC 6600 digital computer. Figure 2 shows a typical scattered-bremsstrahlung spectrum together with a background spectrum measurement. The ordinate scale is logarithmic to emphasize the low background level, which was typically less than 4% of the signal level.

To obtain P from the measured data, the following corrections were applied: (a) The counts in each channel were corrected for Compton scattering of photons out of the detector; (b) the counts were corrected for the escape of Ge fluorescent x rays from the detector using experimentally determined escape-peak–to–photopeak ratios; (c) unpolarized characteristic lines from the target were removed from the spectrum; (d) the counts were corrected channel by channel for the shift in energy due to the Compton scattering in the polarimeter (this correction was nonlinear with photon energy and resulted in a small distortion of spectrum shape); and (e) $P(k/T_0)$ for each T_0, θ, and Z was determined according to Eq. (3) and fit with polynomials of up to fourth order using a least-squares technique.

Results

Experimental results were obtained for 48 combinations of T_0, θ, and Z. Typical polarization results shown in Figs. 3–5 are polynomial fits to the corrected data. Table I lists the coefficients of the polynomials which best fit each experiment.

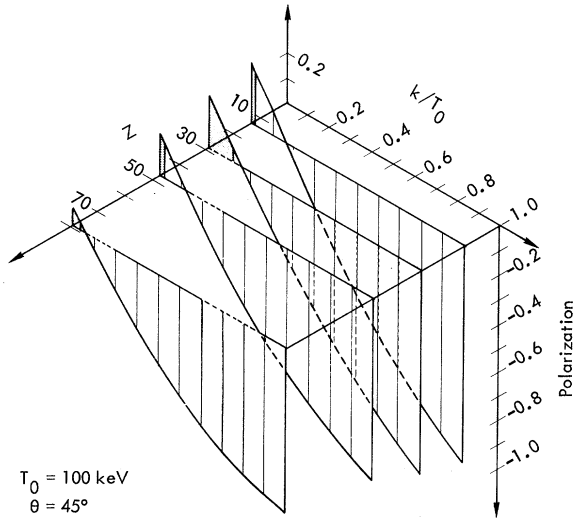

FIG. 3. Linear polarization plotted as a function of relative photon energy k/T_0 for $Z=13$, 29, 47, and 79. Shaded regions indicate extrapolated results. The dashed segments of the k/T_0 grid lines for $Z=29$, 47, and 79 indicate regions from which unpolarized characteristic x rays were removed.

TABLE I. Coefficients of polynomial fits to experimental data $P(k/T_0)=a+b(k/T_0)+c(k/T_0)^2+d(k/T_0)^3$, where k/T_0 = photon energy relative to the incident electron energy.

T_0 (keV)	Z	θ (deg)	a	b	c	d
50	13	22.5	0.0657	−0.525	0.595	−0.866
50	13	45	0.0611	−1.02	0.0655	...
50	13	90	0.0376	−0.995	...	...
50	13	135	−0.138	0.238	0.8175	...
50	29	22.5	−0.0178	0.0316	−0.635	...
50	29	45	0.00919	−0.805	0.012	...
50	29	90	−0.0127	−0.795	...	...
50	29	135	−0.0948	−0.0116	−0.465	...
50	47	22.5	−0.00337	−0.202	−0.0273	...
50	47	45	0.0192	−0.945	0.239	...
50	47	90	−0.0947	−0.630	...	...
50	47	135	−0.121	−0.111	−0.233	...
50	79	22.5	0.0122	−0.415	...	...
50	79	45	−0.102	−0.765	0.2473	...
50	79	90	−0.272	−0.384	...	...
50	79	135	−0.0977	−0.358	−0.0273	...
75	13	22.5	0.0604	−0.421	−0.404	...
75	13	45	0.167	−1.31	0.253	...
75	13	90	0.141	−1.05	...	...
75	13	135	−0.0648	−0.0029	−0.534	...
75	29	22.5	−0.0141	−0.1275	−0.544	...
75	29	45	0.153	−1.22	0.254	...
75	29	90	0.0654	−0.970	...	...
75	29	135	−0.0799	0.124	−0.574	...
75	47	22.5	−0.00343	0.0140	−0.434	...
75	47	45	−0.102	−1.01	0.199	...
75	47	90	−0.0123	−0.780	...	...
75	47	135	−0.219	−0.338	...	...
75	79	22.5	−0.0102	−0.416	...	...
75	79	45	−0.00692	−1.07	0.419	...
75	79	90	−0.209	−0.488	...	...
75	79	135	−0.122	−0.221	...	...
100	13	22.5	0.115	−0.689	−0.170	...
100	13	45	0.266	−1.70	0.547	...
100	13	90	0.136	−1.06	...	...
100	13	135	−0.0746	0.178	−0.732	...
100	29	22.5	0.151	−0.711	0.413	−0.595
100	29	45	0.214	−1.44	0.408	...
100	29	90	0.135	−0.967	...	...
100	29	135	−0.0743	0.0682	−0.439	...
100	47	22.5	0.100	−0.693	...	...
100	47	45	0.187	−1.53	0.628	...
100	47	90	0.0983	−0.924	...	...
100	47	135	−0.489	−0.230	−0.139	...
100	79	22.5	0.0345	−0.577	...	...
100	79	45	0.0736	−1.32	0.576	...
100	79	90	−0.0274	−1.03	0.398	...
100	79	135	−0.0869	−0.330	...	...

Experimental Error

Sources of error contributing to the experimentally determined polarization are considered below.

a. Polarimeter asymmetry correction. The asymmetry correction factor $(R+1)/(R-1)$ ranged between 1.01 and 1.06. A conservative estimate of 25% for the uncertainty in R gave an error in $P<2\%$.

b. Counting statistics and polynomial fit. The errors due to counting statistics and the goodness-of-the-polynomial fit to the final data are both incorporated in the least-squares calculation. These

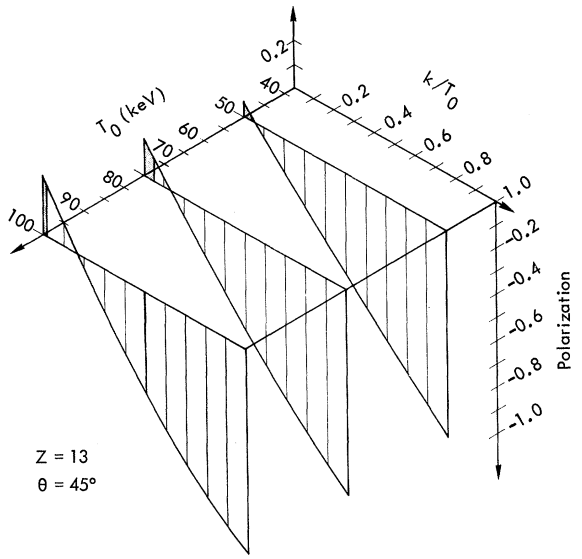

FIG. 4. Linear polarization plotted as a function of relative photon energy k/T_0 for $T_0 = 50$, 75, and 100 keV. Shaded regions indicate extrapolated results.

were less than 1% over most of the spectrum but approached 15% at the end points for backward angles, or where $P \sim 0$ (near polarization cross-over energy).

c. Target thickness. Incident electrons are scattered and lose energy in passing through the target. It is appropriate to consider these sources of error separately.

The result of electron scattering is that the original electron direction is changed, thereby averaging the bremsstrahlung intensity over an angular interval related to the mean angle of elastic electron scattering. For each target and electron energy, this angle was obtained from the plural scattering distribution of Keil *et al.*[28] For 100-keV electrons on Al it was 1.5°, and for 50-keV electrons on Au it was 3.8°. These angles are less than the 7° or 10° angle subtended by the polarimeter. It was estimated that the polarization is lowered by less than 0.5% owing to this effect. Therefore, no correction was made. Kulenkampff and Zinn[24] measured the effect of target thickness on polarization, and their results suggest that a systematic correction of as much as 2% could be made to our results. Since it was not clear to what extent their results apply to the present work, no correction was made.

Energy losses were estimated using the Berger and Seltzer[29] energy-loss tables and were negligible compared to the energy resolution of this experiment.

d. Polarimeter geometry. The finite solid angle subtended by the polarimeter had the effect of broadening the polarimeter energy response and of averaging polarization over a finite spread in emission angle $\Delta\theta$. As seen in Fig. 2, the energy response was sufficiently narrow to introduce negligible error. The $\Delta\theta$ in emission angle was 7° or 10° depending upon polarimeter geometry, and this resulted in a lowering of polarization by as much as 0.5%. This value was determined from the angular dependence of polarization calculated by Tseng and Pratt.[6] No correction was made.

e. Beam current integration. The current integrator was calibrated before and after each experiment and was found to be precise to within 0.5%.

f. Fluorescence escape correction. Escape-peak–to–photopeak ratios for the Ge(Li) spectrometer used in this experiment were measured and were in excellent agreement with ratios for a similar spectrometer.[30] For thin-target bremsstrahlung, the spectrum correction for the escape of Ge x rays from the spectrometer is additive above the Ge K absorption edge and subtractive below. At high photon energy (> 50 keV) the correction was negligible. Between 11 and 50 keV, the correction was less than 3%. Below 11 keV it ranged from 10 to 50%. The contribution to uncertainty in P is a function of the product of the correction and the correction uncertainty. The largest contribution from this effect was ± 5% at 5 keV, where the correction was large and P small.

g. Correction for Compton scattering out of the detector. The magnitude of this correction was a few percent or less in all cases and was determined

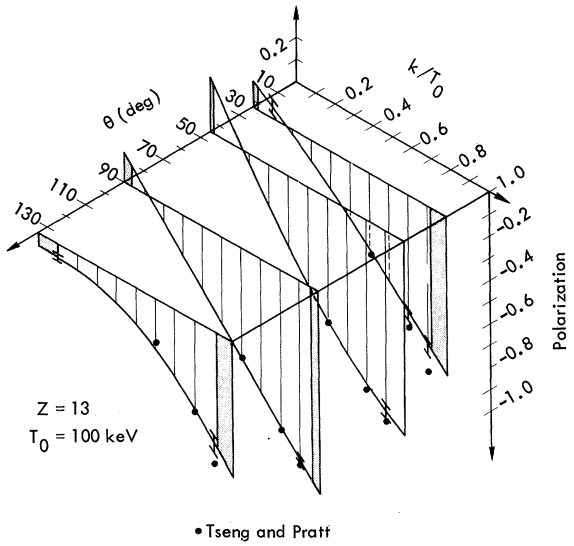

FIG. 5. Linear polarization plotted as a function of relative photon energy k/T_0 for $\theta = 22.5°$, 45°, 90°, and 135°. Shaded regions indicate extrapolated results. Error bars indicate uncertainty. Calculated results of Tseng and Pratt (Ref. 6) are shown.

from the experimental and calculated results of Slivinsky and Smith[31] for a similar detector geometry. The uncertainty in the correction was as large as 50% at low energies. However, since the magnitude of the correction was typically < 2%, the uncertainty in polarization for this effect ranged from zero percent at high energies to < 2% at a few keV.

h. Total error. All of the above errors were considered to be independent and were added in quadrature. Typical uncertainty is indicated by the size of the error bar on some of the data points. The total error ranged from approximately ± 2% to as much as ± 10% at spectrum endpoints for backward angles.

III. DISCUSSION

k Dependence

Low-energy bremsstrahlung is predominantly dipole radiation with the photon electric vector lying in the direction of the electron acceleration vector. When observed at right angles to the incident electron beam direction, high-energy photons ($k/T_0 \sim 1$) are polarized parallel to the emission plane ($P < 0$), while low-energy photons are polarized perpendicular to the emission plane ($P > 0$). At some intermediate photon energy the polarization reverses from positive to negative. When the photons are observed at small forward angles ($\theta \sim 0$) or large backward angles ($\theta \sim \pi$), P should approach zero over the entire spectrum.

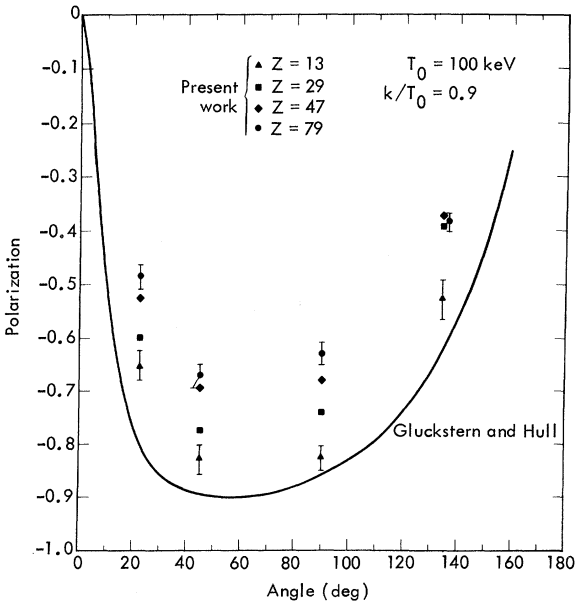

FIG. 6. Linear polarization near the high-energy limit of the spectrum, $k/T_0 = 0.9$, as a function of angle for $T_0 = 100$ keV. Solid line indicates calculated results of Gluckstern and Hull (Ref. 2).

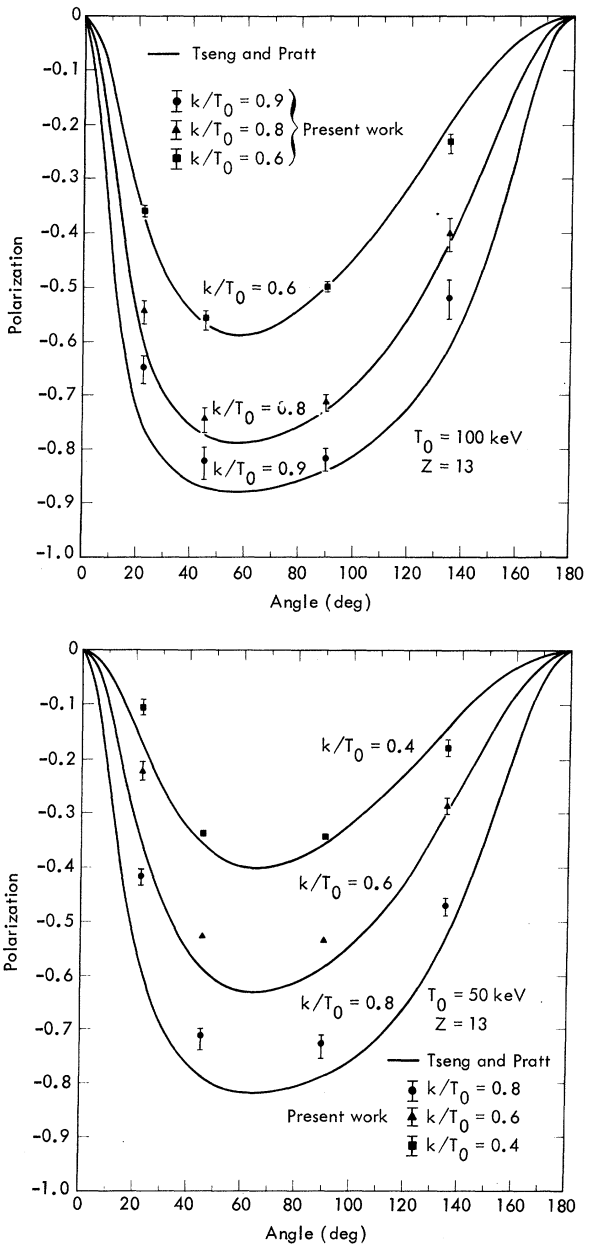

FIG. 7. Linear polarization as a function of angle with parametric dependence upon photon energy k/T_0. Solid lines are calculated results of Tseng and Pratt (Ref. 6).

Motz[21] has measured the bremsstrahlung polarization at an emission angle of 20° for 1-MeV electrons incident on Al and Au targets and found the polarization reversal to occur at $k/T_0 \sim 0.4$. This was slightly lower than the $k/T_0 \sim 0.5$ predicted by Gluckstern and Hull.[2] For the present work, the reversal is predicted by Sommerfeld and by Gluckstern and Hull to occur in the range $0.1 \leq k/T_0 \leq 0.2$. Figures 3–5 show strong parallel polariza-

tion over most of the photon-energy spectrum and a reversal in the range $0.1 \leq k/T_0 \leq 0.15$.

Z Dependence

In bremsstrahlung, the Coulomb field of the nucleus sometimes alters the direction of the incident electron before the photon is emitted. This phenomenon, called the Coulomb effect,[32] results in a decrease in observed polarization. This effect increases with Z indicating that P should decrease with increasing Z. As seen in Fig. 3, the most dramatic dependence of $P(k/T_0)$ upon Z occurs at low photon energy.

T_0 Dependence

The dependence of $P(k/T_0)$ on T_0 is illustrated in Fig. 4. As T_0 increases, the magnitude of the Coulomb effect diminishes, thus increasing both the perpendicular and parallel polarization. Further, as the electron becomes more relativistic, the transverse component of acceleration is enhanced and causes $I_\perp$ to increase at the expense of $I_\parallel$. The net result is a pronounced increase in $P(k/T_0 \sim 0)$ with increasing T_0, and no observable change in $P(k/T_0 \sim 1)$.

θ Dependence

For the low electron energies used in this work, $P(k/T_0)$ is most negative in the range $\frac{1}{4}\pi < \theta < \frac{1}{2}\pi$. As T_0 increases, this will occur at smaller angles because of spin effects.[23]

In Fig. 6 the present results for $P(k/T_0 = 0.9)$ versus emission angle are compared to the theoretical predictions of the Gluckstern–Hull calculation (GH) for $T_0 = 100$ keV. The GH values were taken from Ref. 23 and do not account for screening. The calculated polarization as a function of emission angle agrees qualitatively with experiment, but is higher.

Comparison of present results to predictions of Tseng and Pratt[6] have been made in the few cases for which their results were available ($Z = 13$ and 79, $T_0 = 50$, 75, and 100 keV). Two of these cases are shown in Fig. 7. In general, reasonable agreement was obtained for $T_0 = 100$ keV, but for lower electron energies, the calculated polarization is consistently higher than experiment.

Haug[4] has calculated the polarization at the high-energy limit of the spectrum ($k/T_0 = 1$) for $T_0 = 100$ keV and $Z = 4$, 13, and 79, assuming an unscreened nucleus. Figure 8 shows Haug's results to be in reasonable agreement with experiment for $Z = 79$. For lower Z, the experimentally determined polarization is less than predicted at $\theta = 22.5°$ and 135°.

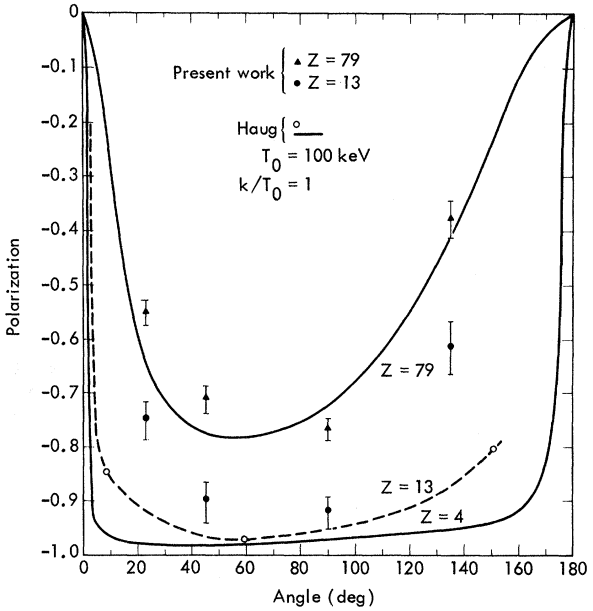

FIG. 8. Linear polarization at the high-energy limit of the spectrum, as a function of angle for $T_0 = 100$ keV. The dashed line connects points calculated by Haug for $Z = 13$. The solid lines were calculated by Haug for $Z = 4$ and $Z = 79$.

Comparisons with predictions based on Sommerfeld's[5] theory, either directly as calculated by Kirkpatrick and Wiedmann[1] or as relativistically transformed by Kulenkampff *et al.*,[33] were generally poor, since Sommerfeld did not include screening or relativistic effects.

ACKNOWLEDGMENTS

We thank Don E. Smith, who wrote the data-analysis codes, and John Lietzke, who performed mechanical design and fabrication. Thanks are also due to H. K. Tseng and R. H. Pratt, who provided their bremsstrahlung code for our use prior to publication. One of the authors (RWK) would like to thank Professor S. D. Bloom for his interest in and support of this thesis research.

*Work performed under the auspices of the U.S. Atomic Energy Commission and submitted by one of us (RWK) in partial fulfillment of the Ph.D requirement of the Department of Applied Science of the University of California at Livermore.

[1] P. Kirkpatrick and L. Wiedman, Phys. Rev. **67**, 321 (1945).
[2] R. L. Gluckstern and M. H. Hull, Jr., Phys. Rev. **90**, 1030 (1953).
[3] H. Olsen and L. C. Maximon, Phys. Rev. **114**, 887 (1959).
[4] E. Haug, Phys. Rev. **188**, 63 (1969).
[5] A. Sommerfeld, Ann. Phys. (N.Y.) **11**, 257 (1931).
[6] H. K. Tseng and R. H. Pratt, Phys. Rev. A **3**, 100 (1971); also private communication.
[7] G. C. Barkla, Philos. Trans. R. Soc. Lond. **204**, 467 (1905).
[8] E. Bassler, Ann. Phys. (N.Y.) **28**, 808 (1909).
[9] L. Vegard, Proc. R. Soc. Lond. **83**, 379 (1910).
[10] P. Kirkpatrick, Phys. Rev. **22**, 226 (1923).
[11] G. A. Ross, J. Opt. Soc. Am. **16**, 375 (1928).
[12] E. Wagner and P. Ott, Ann. Phys. (N.Y.) **85**, 425 (1928).

[13]H. Kulenkampff, Z. Phys. 30, 513 (1929).
[14]B. Dasannacharya, Phys. Rev. **35,** 129 (1930).
[15]Y. F. Cheng, Phys. Rev. **46,** 243 (1934).
[16]D. S. Piston, Phys. Rev. **49,** 275 (1936).
[17]B. F. Boardman, Phys. Rev. **60,** 163 (1941).
[18]V. W. Slivinsky, Bull. Am. Phys. Soc. **16,** 546 (1971).
[19]W. Duane, Proc. Natl. Acad. Sci. USA **15,** 803 (1929).
[20]H. Kulenkampff, S. Leisegang, and M. Scheer, Z. Phys. **137,** 435 (1954).
[21]J. W. Motz, Phys. Rev. **104,** 557 (1956).
[22]J. W. Motz and R. C. Placious, Phys. Rev. **112,** 1039 (1958).
[23]J. W. Motz and R. C. Placious, Nuovo Cimento **15,** 571 (1960).
[24]H. Kulenkampff and W. Zinn, Z. Phys. **161,** 428 (1961).
[25]F. Huffman, Ph.D. thesis (Johns Hopkins University, 1964) (unpublished).
[26]M. Scheer, E. Trott, and G. Zahs, Z. Phys. **209,** 68 (1968).
[27]R. W. Kuckuck, Lawrence Livermore Laboratory, Report No. UCRL 51188, 1972 (unpublished).
[28]E. Keil, E. Zeitler, and W. Zinn, Z. Naturforsch. A **15,** 1031 (1960) [translated in UCRL-Trans-1036 (1964)].
[29]M. J. Berger and S. M. Seltzer, NAS-NRC Publication No. 1131, 1964 (unpublished); also NASA Report No. NASA SP-3012, 1964 (unpublished).
[30]V. W. Slivinsky and P. J. Ebert, Nucl. Instrum. Methods **71,** 346 (1969).
[31]V. W. Slivinsky and D. E. Smith (private communication).
[32]H. W. Koch and J. W. Motz, Rev. Mod. Phys. **31,** 920 (1959); and Ref. 23.
[33]H. Kulenkampff, M. Scheer, and E. Zeitler, Z. Phys. **157,** 275 (1959).

PHYSICAL REVIEW A VOLUME 7, NUMBER 2 FEBRUARY 1973

Direct Measurement of the Ratio between the Transfer Rates of Muons from μp and μd Atoms to Xenon in a Gaseous Target of Deuterated Hydrogen

A. Bertin, M. Bruno, and A. Vitale
Istituto di Fisica dell'Università di Bologna and Istituto Nazionale di Fisica Nucleare, Sezione di Bologna, Italy

A. Placci and E. Zavattini
CERN, Geneva, Switzerland

(Received 12 September 1972)

The ratio B between the transfer rates $\lambda_{\mu p,\mathrm{Xe}}$ and $\lambda_{\mu d,\mathrm{Xe}}$ of muons from μp and μd muonic atoms to xenon has been directly measured by stopping negative muons in a gaseous target containing deuterated hydrogen and small xenon admixtures at a total pressure of 6 atm abs. and at 293 °K. The results were obtained by analyzing the differential time distribution of the decay electrons coming from muons stopped within the gaseous mixture. In this way one gets $B = 1.98 \pm 0.12$, which supports the dependence of the transfer rates on the mass of the primary muonic atom within 6%. More precise values for $\lambda_{\mu p,\mathrm{Xe}}$ and $\lambda_{\mu d,\mathrm{Xe}}$ are also given, i.e., $\lambda_{\mu p,\mathrm{Xe}} = (4.53 \pm 0.15) \times 10^{11}$ sec^{-1} and $\lambda_{\mu d,\mathrm{Xe}} = (2.30 \pm 0.17) \times 10^{11}$ sec^{-1}. A lower limit for the scattering cross section σ of μd atoms against xenon is obtained, i.e., $\sigma \geq 10^{-15}$ cm^2.

I. INTRODUCTION

The atomic and molecular processes which negative muons undergo in hydrogen and deuterium were widely investigated because of their close relation with the muonic catalysis of nuclear reactions[1] and with the nuclear capture of muons by protons[2,3] and deuterons.[4,5]

Among these phenomena, particular interest was devoted to the study of the transfer reactions of muons from μp and μd atoms to other elements ${}_ZY$ (Z being the atomic number),

$$\mu p + {}_ZY \rightarrow \mu\, {}_ZY + p\,, \tag{1}$$

$$\mu d + {}_ZY \rightarrow \mu\, {}_ZY + d\,, \tag{2}$$

which may occur at large rates if the hydrogen or deuterium is contaminated by even a small amount of ${}_ZY$.

A theoretical analysis of process (1) was carried out by Gershtein.[6] Quite generally, he found that large rates are to be expected for reaction (1) due to the existence of *crossing points* of the molecular terms corresponding to charge exchange in the $(\mu p + {}_ZY)$ system. More specifically, he showed that approximate predictions of the algebraic form of the rate $\lambda_{\mu p,Y}$ for reaction (1) can be obtained, provided the kinetic energy T of the μp muonic atom satisfies either one of the following conditions:

$$T \ll 0.12/(M^2Z^2)\,, \tag{3}$$

$$T \gg 0.12/(M^2Z^2)\,. \tag{4}$$

The energies are given here in μ-atomic units, and M is roughly equal to the mass of the μp muonic system in units of the muon mass.

Experimental results on the rates of process (1) for several ${}_ZY$ elements were obtained by different techniques,[7–12] confirming the large rates predicted by Gershtein. However, only a few measure-

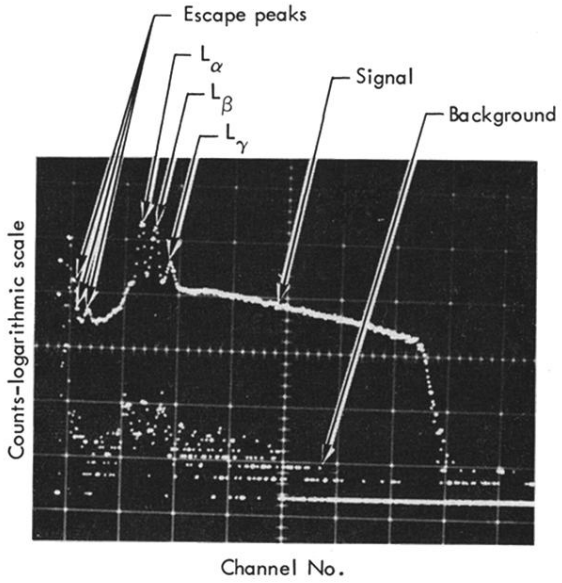

FIG. 2. Photograph of scattered spectrum showing signal and background levels for $T_0 = 50$ keV, $Z = 79$, $\theta = 135°$, and polarimeter positioned parallel to reaction plane. Ordinate scale is logarithmic: each division is approximately a factor of 10.